

CONSTITUTIVE MODELLING AND PARAMETER IDENTIFICATION FOR RUBBER-LIKE MATERIALS

Z. N o w a k

**Polish Academy of Sciences,
Institute of Fundamental Technological Research
Department of Mechanics of Materials
Świętokrzyska 21, 00-049 Warszawa, Poland**

The aim of the paper is to determine the phenomenological model to characterize the stress-strain relation and to simulate the behaviour of solid polyurethane (PUR) rubbers used in civil engineering, as well as to present the process of identification of model parameters for such materials. For the material studied the strain energy density function was established and a general constitutive relationship for the second-order tensor of Piola–Kirchhoff stress for elasticity is determined. Constitutive relationships for engineering stress in terms of the principal stretches are also specified. The paper presents the method of identification of parameters for constitutive models of hyperelasticity and hypoelasticity for the accessible experimental data. The applied identification procedure is based on the feature of two-phase structure of polyurethane material and is supported by the experimental data from uniaxial quasi-static tension and compression tests. In the analysis, the material behaviour was considered both for the case of incompressible deformation and also for the case of slightly compressible, non-linearly elastic materials that are homogeneous and isotropic. The change of volume was admitted too, in range of large deformations in a tension and compression test. The attempt of description of stress-softening phenomenon was undertaken in rubber-like materials, for a given level of strain, under unloading (the Mullins effect) caused by the damage of microstructure of this material. Different descriptions of the stress-softening phenomenon were already proposed in the literature but they fail to give fully satisfactory conformity of experimental data with theoretical predictions. The phenomenological model by ELIAS–ZÚÑIGA and BEATTY, *A new phenomenological model for stress-softening in elastomers*, ZAMP, **53**, 794–814, 2002, for such materials was modified by different softening functions and a simplified version of this model was identified, based on the experimental data. In the proposed model, the damage of microstructure was described by a new exponential function, which depends on the current magnitude of intensity of strain and its earlier maximum value during the process of material loading. In this paper, a suitable analysis of existent models and their verification based on experimental data for polyurethane rubber is presented for uniaxial experiments. It is shown that the magnitude of stress-softening varies with strain and this phenomenon increases with the magnitude of the pre-strain and the type of loading: monotonic tension, compression or cyclic loading. The obtained results are presented graphically for uniaxial tension and compression.

Key words: rubber-like material, hyperelastic constitutive model, damage of polyurethane rubber.

1. INTRODUCTION

Polyurethane (PUR) materials, among other polymers and elastomers, exhibit high elasticity combined with high friction resistance what results in a wide array of applications, e.g. as engine mounts, bump stoppers or flexible seismic isolator pads. Polyurethanes are randomly segmented copolymers (QI and BOYCE [45], KRÓL [46]), composed of hard and soft segments forming a two-phase microstructure. The hard domains are immersed in a rubbery soft segment matrix (KRÓL [46]) and, depending on the hard segment content, the morphology of the hard domains changes from one of the isolated domains to one of the interconnected domains. Phase separation occurs in most PUR due to the intrinsic incompatibility between the hard segments and soft segments: the hard segments, composed of polar materials, can form carbonyl to amino-hydrogen bonds and thus, tend to cluster or aggregate into ordered hard domains, whereas the soft segments form the amorphous domains. The presence of hard domains in segmented polyurethanes is very important for their mechanical properties. In segmented polyurethanes, hard domains act as physical crosslinks, playing a role similar to chemical crosslinks in vulcanizates and imparting the material's elastomeric behaviour. Since hard domains also occupy significant volume and are stiffer than the soft domains, they also play the role of effective nano-scale fillers and render a material behaviour similar to that of a composite (KRÓL [46]). At room temperature, soft domains are above their glass transition temperature and impart the material its rubber-like behaviour; hard domains are below their glassy or melting transition temperature and are supposed to govern permanent deformation, high modulus and tensile strength. The domain structure also imparts PUR's versatility in mechanical properties. A wide variety of property combinations can be achieved by varying the molecular weight of the hard and soft segments, their ratio and chemical type. At present, polyurethane materials form an important group of products because of their advantage in chemical resistance and excellent mechanical properties.

It is well known that rubber-like materials exhibit a strongly non-linear behaviour, characterized by large strain and a non-linear stress-strain behaviour under static conditions. Under cyclic loading conditions the stress-softening phenomena are observed. The stress-softening phenomenon, also called the Mullins effect, is characterized by an important loss of stiffness during the first cycles of fatigue experiments. More precisely, the Mullins effect is defined as a strain-induced stress-softening of the material, that takes place after the first monotonic loading path of loading cycles. Most of the hyperelastic models of elastomers assume that the Mullins effect takes place during the first cycle of loading and that it depends only on the maximum strain endured previously by the material. These prerequisites are quite acceptable in view of experimental observations.

As the physical foundations of the phenomenon are not well established, a majority of studies propose phenomenological constitutive equations. Many authors use the thermodynamical framework of Continuum Damage Mechanics (CDM), which was extended to the case of elastomers in order to simulate the Mullins effect.

The general three-dimensional case on the subject is due to SIMO [22] who derived a large-strain viscoelastic constitutive equation with damage for rubber-like materials. This model was improved by introducing microscopic concepts by GOVINDJEE and SIMO [23]. More recently, several authors developed phenomenological hyperelastic models with damage to describe the Mullins effect in engineering applications (DE SOUZA NETO *et al.* [11]; MIEHE [27]; MIEHE and KECK [47]; DE SIMONE *et al.* [39]). Another approach used to develop constitutive equations for the Mullins effect is based on the two-phase model of MULLINS and TOBIN [24]. These concepts postulate that the polymer network evolves under deformation; they assume that parts of the network are broken and others are deformed during loading. In this approach, the stress should be corrected by a scalar deformation function that depends on the given measure of deformation, expressed as a scalar function of the principal invariants of the left Cauchy–Green tensor.

Similarly, BEATTY and KRISHNASWAMY [16] derived a constitutive equation that generalized the previous papers by JOHNSON and BEATTY [15] on particular deformation states. In this work, the two-phase theory of MULLINS and TOBIN [24] is considered, and the transformation of hard regions into soft regions is entirely controlled by a stress-softening function, that depends on the maximum strain previously endured by the material. This function corrects the strain-energy function under loading; a different form of it was recently proposed by ELIAS–ZÚÑIGA and BEATTY [17]. The paper presented by OGDEN and ROXBURGH [19] applied an approach which differs from the aforementioned theories because the stress-softening function (that depends on the maximum strain energy endured by the material) is activated only on unloading paths. This theory greatly simplifies the identification of material parameters, but it does not respect the physical phenomenon of network changes during loading. The constitutive equations based on network evolution are more specific for polymers than CDM, but the corresponding thermodynamical framework is not well-defined. Nevertheless, it appears that the constitutive equations obtained by the two approaches, i.e. CDM and the network evolution, are similar. More complex models based on viscoelasto-plastic theories have been also proposed as, for example, in the papers by LION [40], SEPTANIKA and ERNST [41] and ANDRIEUX and SAANOUNI [42].

There is no general agreement on the explanation of the microscopic and mesoscopic origins of the Mullins effect. MULLINS [26] suggested that stress soft-

ening in two-phase elastomers is due to the breakdown of interactions between the filler particles and the rubber matrix. The mesoscopic properties of real materials, however, are not uniform, and the polymerization process generates non-uniformity in the distances between the filler particles. The interactions between the phases suggests that after the primary loading, the material structure must be more complex than in the virgin state in which the chains are short. This condition is a necessary condition for prediction of the stress softening. It is not, however, a special feature of the MULLINS [26] or ELIAS–ZÚÑIGA and BEATTY [17] models, and it must also hold for any model with limited chain extensibility. For example, the model used by MARCKMANN *et al.* [43] based on the eight-chain Arruda–Boyce model exhibits the same effect. The model presented by HORGAN *et al.* [12] suggests that during the primary loading, degradation of the material occurs. It is possible that as degradation continues, a rearrangement of the network, involving displacement of network junctions, may also take place.

The main objective of this paper is to identify the phenomenological model of the polyurethane elastomer materials used in the civil engineering and railway industry. Here, the emphasis is laid on models that can be implemented in finite-element software and used for engineering applications. The mechanical behaviour of a representative PUR material is studied in a series of uniaxial tension and compression tests, investigating cyclic loading effects on the large-strain deformation behaviour. A constitutive model for the observed stress-strain behaviour is then developed and compared directly to experimental data. Both the monotonic uniaxial tension loading and uniaxial compression and subsequent unloading curves are examined. The experimental data presented recently by KWIECIEŃ and ZAJĄC [20] and KWIECIEŃ *et al.* [21], exhibit a non-monotonic variation of stress softening with the extent of deformation. The analysis of experimental results has also shown that the property of stress softening in polyurethane elastomer strongly depends on the magnitude of pre-strain. Uniaxial tension and compression examples are presented in order to highlight the influence of the loading path on the material behaviour. The identification of material parameters for uniaxial monotonic loading leads to a good qualitative agreement for both the uniaxial tensile and compression conditions. As most of the phenomenological models developed for the Mullins effect are based on the microstructural damage of the JONHSON and BEATTY [15] theory, it is of great importance to rationalize its use and to exhibit its advantages and limitations in this context.

This paper is restricted to hyperelasticity with isotropic damage. Cyclic compression experimental data are used to construct the evolution equation of the stress-softening variable and to exhibit some limitations of this approach. The emphasis is laid on the restrictions of the damage theory as applied to the Mullins effect with respect to physical phenomena, and on the choice of the damage soft-

ening function and criterion. The corresponding analysis for different forms of softening functions appearing in constitutive models are considered and the results for the axial tests are presented. The new forms of the softening function assumed in our model of the Mullins effect aim to explain the difficulties in fitting the data by models which were formulated by OGDEN and ROXBURGH [19], ELIAS-ZÚÑIGA and BEATTY [17], QI and BOYCE [45] and others.

We begin in Sec. 2 with a brief description of physical aspects of the internal damage of rubber-like materials with micro-phase separation. In Sec. 3, the constitutive framework is presented. The emphasis is laid on the uniaxial tension and compression. Section 4 is devoted to the experimental results for polyurethane elastomers. The parameters identification process, as the integral part of constitutive modelling, are presented and discussed in Sec. 5 and the conventionally represented uniaxial experimental data are reanalysed in a manner consistent with the theory.

The numerical part of the identification work for uniaxial cycle loading with Mullins effect is presented in figures in Sec. 6. We concentrate on the Mullins effect and we are not concerned with hysteresis, residual strain, thermal and viscoelastic effects. The proposed model is purely phenomenological and does not take into account the physical structure of the material; hence it can be applied to any material exhibiting the Mullins effect. We assume that the virgin material is isotropic with respect to an undeformed and unstressed state. In Sec. 6.1 we define the terms damage function, which depends on the principal stretches, and damage point, which depends on the principal directions and the history of the right stretch tensor. Finally, the concluding remarks are given in Sec. 7.

2. PHYSICAL ASPECTS OF INTERNAL DAMAGE OF RUBBER

2.1. *Micro-phase separation in polyurethane elastomers*

The specific structural feature of high-molecular weight polyurethane elastomers, is their segmented structure. The PUR chain is composed of hard segments and soft segments arranged alternately. The structure of the segmented PUR was already schematically presented and such schemes are presented in [28–30, 42]. The structure of a PUR macro-molecule results from the spatial arrangement of polymer chains in the condensed phase, i.e. after the polymerisation process and possibly after cross-linking. Considerable structural diversification of PUR chains gives rise to strong interactions, both within individual macro-molecules and between different macro-molecules. The hard segments can interact with each other. That phase is hardly miscible with the soft phase which has been formed with the use of much less polar, soft segments. If the hard phase and soft phase within a PUR become completely immiscible, two separate

phase transition points can be frequently observed as two clearly different glassy temperatures for soft segments and for hard segments. That is specific just for segmented PUR elastomers.

In some cases, additional crystalline phases can form within each of those phases. The interactions through hydrogen bonds can also create separate hard domains within the soft phase or separate soft domains within the hard phase. That certainly produces a multi-phase system in which usually the continuous soft phase makes the matrix. The matrix is penetrated through by some part of the hard phase or by the whole of it. Alternatively, the hard phase can be dispersed in the matrix. Separation of micro-phases is not precise, however, and some hard segments are dispersed within the domains of soft segments and the intermediate phase is thus formed. The degree of phase separation in PURs is controlled by numerous factors: chemical structure of PUR chains, polarity of their structural fragments, sizes of hard segments and soft segments, molecular weights and molecular weight distribution in PURs, the method employed to shape the final PUR product (bulk, foil, fibre) and process parameters adopted for that method (temperature, melt cooling rate, solvent evaporation rate, possible presence or absence of mechanical stresses). From the theoretical viewpoint, phase separation can be controlled by the thermodynamic factors which result from differences in the structures of hard segments and soft segments, and by kinetic factors which for example promote separation of some segments due to their higher mobility, and thus with lower viscosity of the reaction mixture which is just polymerizing. The micro-phase separation is generally more prominent in polyurethanes due to stronger interactions between ester groups and urethane groups than between ether groups and urethane groups.

2.2. Intermolecular interactions. Elastomer phase structure

The fundamental static properties for PUR elastomers materials are defined by Young's modulus E , shear modulus G and by unit elongation and Poisson's ratio $\nu = 0.3 - 0.5$. The static properties also involve hardness resistance. The mechanical properties of the parent material will be decided by the structures of PUR chains and by the phase structures of PURs. That problem has been extensively described in literature since mechanical properties affect directly the range of applicability of PUR elastomers and PUR coatings. Polyurethane materials behaviour under quasi-static loads is determined by the elastomer phase structure, and that in turn is controlled by the organisation of its segments. In polyurethane materials, the mechanical properties make the resultant of structural factors and physical chemical interactions such as like size and flexibility of hard and soft segments, ability to form hydrogen bonds, van der Waals force, entanglement of chains, orientation of segments, cross-linking bonds, micro-phase separation

and content of crystalline phase. The most important contribution comes from the chemical structure and from the size and structure of hard and soft segment resulting from this.

The sizes of hard segments increase when the number of those segment increases. Initially, they form a system of separate islands which do not contact each other and are dispersed within the matrix of soft segments. Above a certain limit number, some of them start to touch each other, what forms the system of hard domains. Further increase in the number of hard segments favours their association and the roles of phases become opposite. Both the cohesion energy and hydrogen bonds in hard domains are higher than in soft domains. Hence, the role of hard domains is sometimes compared to that of a filler material which is used to reinforce the elastomer structure and to improve its mechanical properties: in particular, its strength and hardness. On the other hand, higher elasticity is favourable for intermolecular interactions. In contrast to mechanical strength, which is controlled first of all by the structure of hard segments, elasticity is affected mainly by soft segments. The capacity for crystallisation of phases, which is conditioned by the structural regularity, contents of individual segments and efficient phase separation, is favourable for higher tensile strength, tearing strength, hardness and higher stresses at the predefined elongation levels. The mechanical properties of PURs can be also considerably affected by the method adopted for the final treatment of the product, like soaking or racking. That increases the phase separation and orderly arrangement of elastomer within its crystalline structures, i.e. elastomer strength is advantageously improved in that way (see POMPE *et al.* [48]).

2.3. *The role of a damage parameter*

Although rubbery-like materials may be regarded as purely elastic, damaging does take place due to straining. The internal degradation in this case is mainly characterized by rupture of the molecular bonds, concentrated in regions containing impurities and defects. In general, the damage response of such materials is predominantly brittle. In rubber-like materials, even at very small overall straining, damage can occur in the form of progressive breakage of shorter polymer chains. In Sec. 6.2 we have shown that it is convenient to introduce a damage parameter to describe the evolution of alteration of the network. This can be done in a purely empirical way, and this is the approach used by Beatty and co-workers in several publications (BEATTY and KRISHNASWAMY [16]; ELIAS-ZÚÑIGA and BEATTY [17] and references contained therein) and also by MARCKMANN *et al.* [43]. First of all, it is possible to use the theory of pseudo-elasticity as proposed by OGDEN and ROXBURGH [19]. In this theory it is assumed that the material response of the body can be described in terms of a pseudo-energy function,

defined per unit volume, of the form $W(f(I), \alpha)$, where α is a damage parameter and $f(I)$ is a function of invariants I_1 , I_2 and I_3 of the deformation tensor. (The role of α here is somewhat different from that of the damage parameter α introduced in Sec. 6.2). In this case it is no longer appropriate to regard W as a stored energy because, through α , irreversible effects are accounted for.

It is often convenient to regard shear modulus for the i th-cycle loads μ_i as functions of a damage parameter, here denoted by α , such that $\alpha \in [0, 1]$, where 0 is associated with the original material and 1 with the fully damaged material (this is a normalization of the scale). The fully damaged material corresponds to an asymptotic state in which no further damage is caused by stress-strain cycling with increasing number i .

3. CONSTITUTIVE MODELS FOR RUBBER ELASTICITY

The elastic properties of rubber-like materials are usually represented in terms of a strain-energy function, denoted by W and defined per unit reference volume (see, for example, BEATTY and KRISHNASWAMY [16]; OGDEN [6–8]). The state of strain in the material is characterized by a tensor measure of deformation, such as the left Cauchy–Green deformation tensor \mathbf{B} . Several forms for the strain energy function of rubber-like materials have been proposed since 1940 in the literature. These can be grouped into those dealing with incompressible materials and those extended to deal with compressibility. They can further be split, depending on the material group being modelled, whether for example the material under consideration is rubber, polymer or foam. The most widely cited strain energy expressions are the Mooney–Rivlin, OGDEN [cf. 6–7] and Blatz and Ko (see e.g. KRISHNASWAMY and BEATTY [31]) models. However, for different strain energy functions, mainly two different kinds of models can be identified.

The first kind is based on experimental observations and phenomenological considerations. The corresponding models are both mathematically simple and quite efficient (OGDEN [6, 7]). The second group of models were developed by considering the physics of the elastomer network. First, conformations of a single polymer chain are determined; then, the behaviour of the whole network is derived using statistical developments. For small and moderate strains, the neo-Hookean (TRELOAR [52]) and the phantom (JAMES and GUTH [53]) models can be mentioned. For large strains, the stretching limit of chains is taken into account and non-Gaussian statistics are employed (TRELOAR and RIDING [54]; ARRUDA and BOYCE [55]; WU and van der GIESSEN [56]). The use of these models reduces the number of relevant material parameters because of their physical foundations, but their mathematical derivations are more complicated than those of phenomenological constitutive equations. For a complete review of the constitutive models for rubber elasticity, the reader can be referred

to OGDEN *et al.* [34], LAMBERT–DIANI and REY [1] or BOYCE and ARRUDA [57]. It has to be mentioned that the present approach can be easily applied to every form of the strain energy function. In the present study, the emphasis is laid on identification of the model with stress-softening phenomenon for the available macroscopic uniaxial loading experimental data only, so that a simple phenomenological strain energy function is chosen.

3.1. The strain energy function for rubber

The hyperelastic materials are described under assumption of existence of the potential of energy of strain $W(\lambda)$, by which the stored strain energy on unit initial volume fraction as a function of strains is defined in the material. In literature, different forms of strain energy potentials are proposed, depending on the form of constitutive model, e.g. Mooney–Rivlin or Ogden. The strain energy function W can be expressed as a function of invariants of a deformation tensor I_1 , I_2 and I_3 . If the left Cauchy–Green deformation tensor \mathbf{B} is employed as the deformation tensor, the deformation invariants can be rewritten in terms of the principal stretches λ_i ($i = 1, 2, 3$),

$$\begin{aligned}
 I_1 &= \text{tr}\mathbf{B} = \lambda_1^2 + \lambda_2^2 + \lambda_3^2, \\
 (3.1) \quad I_2 &= \frac{1}{2}\{(\text{tr}\mathbf{B})^2 - \text{tr}(\mathbf{B}\mathbf{B})\} = (\lambda_1\lambda_2)^2 + (\lambda_2\lambda_3)^2 + (\lambda_3\lambda_1)^2, \\
 I_3 &= \det(\mathbf{B}) = J^2 = (\lambda_1\lambda_2\lambda_3)^2.
 \end{aligned}$$

When the material is incompressible, the third invariant $I_3 = 1$, and W is represented as a function of I_1 and I_2 only, $W = W(I_1, I_2)$. In the case of isotropic elastic incompressible virgin materials, $W = W_0$ and the general expansion of W_0 is considered in the form:

$$(3.2) \quad W_0 = C_{ij}(I_1 - 3)(I_2 - 3)$$

in which C_{ij} ($i, j = 1, \dots, n$) are the material parameters. Several phenomenological models were derived by truncating the series of Eq. (3.2). In order to satisfactorily reproduce the large strain response of the material, the Mooney–Rivlin model is adopted (cf. ELIAS–ZÚÑIGA and BEATTY [17]). The corresponding strain energy function is given by

$$(3.3) \quad W_0 = \sum_{i=1}^3 C_{i0}(I_1 - 3),$$

where C_{10} , C_{20} and C_{30} are the three material parameters. As this model depends only on the first principal invariant, it is not well-adapted to moderate

strain because it does not improve the Gaussian theory. Nevertheless, its mathematical simplicity and ability to reproduce the whole behaviour of elastomers are sufficient qualities for the present study.

Some of the simplest incompressible models proposed in the literature involve a strain-energy function of the form $W_0 = f(I_1)$, and are called generalized neo-Hookean models. In the molecular theory of elasticity, these models involve the introduction of a (non-Gaussian) distribution function, denoted φ , for the end-to-end distance of the polymeric chain. By contrast, a Gaussian distribution function for φ is associated with the special case corresponding to the classical neo-Hookean model

$$(3.4) \quad W_0^H = \mu(I_1 - 3)$$

for incompressible materials, where μ ($\mu > 0$) is the shear modulus in the reference configuration.

In the framework of the phenomenological theory, similar models have been developed by considering the idea of limiting chain extensibility, i.e. by considering strain-energy functions that have a singularity when the first invariant I_1 reaches a certain finite value. The simplest model with limiting chain extensibility is due to GENT [58], who proposed the strain-energy function

$$(3.5) \quad W_0^G(I_1) = -\frac{1}{2}\mu J \ln \left(1 - \frac{I_1 - 3}{J} \right),$$

where μ is again the shear modulus in the reference configuration and $J > 0$ is the constant limiting the value of $(I_1 - 3)$ that accounts for limiting polymeric chain extensibility. In the limit as the chain-extensibility parameter tends to infinity ($J \rightarrow \infty$), Eq. (3.5) reduces to Eq. (3.4), cf. HORGAN *et al.* [12]. From a phenomenological point of view, limiting chain extensibility may be introduced in many ways, and a detailed review of some of the possibilities may be found in HORGAN *et al.* [12] or HORGAN and SACCOMANDI [44].

All the strain-energy functions considered in constitutive modelling will be assumed to satisfy the following conditions: 1. The strain energy is zero in the reference configuration; 2. The stress is zero in the reference configuration; 3. The strain-energy function is positive definite. The specific form of strain-energy densities used to model our rubber-like material behaviour in Sec. 5 and 6 are given in the following subsections.

3.1.1. The Mooney–Rivlin model. The potential in the Mooney–Rivlin model is usually presented for incompressible hyperelastic materials in the following form (see e.g.: [6, 8]):

$$(3.6) \quad W_0^M = C_{10}(\bar{I}_1 - 3) + C_{01}(\bar{I}_2 - 3),$$

where W is the strain energy in unit initial volume fraction, C_{10} and C_{01} are two parameters and \bar{I}_1 and \bar{I}_2 are the first and second invariants of strain deviator defined in terms of the deviatoric principal stretches $\bar{\lambda}_i$ which have the forms (cf. [2, 3, 8, 9])

$$(3.7) \quad \bar{I}_1 = \bar{\lambda}_1^2 + \bar{\lambda}_2^2 + \bar{\lambda}_3^2 \quad \text{and} \quad \bar{I}_2 = \bar{\lambda}_1^{(-2)} + \bar{\lambda}_2^{(-2)} + \bar{\lambda}_3^{(-2)},$$

where $\bar{\lambda}_i = \lambda_i J^{(-\frac{1}{3})}$ and λ_i are principal stretches of the total strain tensor.

Initial shear modulus μ_0 in the Mooney–Rivlin model is defined by

$$\mu_0 = 2(C_{10} + C_{01}).$$

3.1.2. The standard Ogden model. Among the hyperelastic models, in case of polyurethane materials, the OGDEN model (cf. [6, 7]) gives good results; this will be the basis of the model elaborated and which takes into account the material damage. In the case of incompressibility, the strain energy function is presented in the form ([6, 7, 8]):

$$(3.8) \quad W_0^{\text{Og}} = \sum_{i=1}^N \frac{2\mu_i}{\alpha_i^2} \left(\bar{\lambda}_1^{\alpha_i} + \bar{\lambda}_2^{\alpha_i} + \bar{\lambda}_3^{\alpha_i} - 3 \right),$$

where μ_i and α_i are material parameters and N is the number of material parameters (in practice $N \leq 6$), usually $N = 1$. Initial shear modulus μ_0 in Ogden model is defined by

$$(3.9) \quad \mu_0 = \sum_{i=1}^N \mu_i.$$

From the general form of strain energy potential of the Ogden model we can obtain also the peculiar material discussed above, e.g.: Mooney–Rivlin, by special selection of μ_i and α_i .

In the above constitutive description, the coefficient of change of length λ_i ($i = 1, 2, 3$) can be defined as

$$(3.10) \quad \lambda_i = l_i/L = (L + \Delta l_i)/L,$$

where $\Delta l_i = l_i - L$ is the change of length in direction i .

3.2. The standard hypoelastic model

In literature, for description of rubbery-like materials behaviour was also used, different from the previous one, an objective hypoelastic rate model which can be presented by the following formula:

$$(3.11) \quad \overset{\circ}{\mathbf{T}} = 2\mu\mathbf{D} + \lambda^* \text{tr}(\mathbf{D})\mathbf{I},$$

where $\overset{\circ}{\mathbf{T}}$ is an objective measure of rate of the Cauchy stress \mathbf{T} , \mathbf{D} is the rate of stretching (deformation) tensor and it is the symmetric part of the velocity gradient tensor, \mathbf{I} is the unit tensor and μ and λ^* are elastic material constants. For a hypoelastic constitutive equation, in case of uniaxial tension (compression) along direction-11, when $\lambda_2 = (\lambda_1)^{-\nu}$ (for incompressible elastic materials) and if we use logarithmic strain measure, the following formula is obtained:

$$T_{11} = E \ln(\lambda_1),$$

where E is elastic modulus and ν is Poisson's ratio.

Nominal stress in hypoelasticity is given by

$$(3.12) \quad \frac{P}{A_0} = E (\lambda_1)^{-2\nu} \ln(\lambda_1),$$

where A_0 is the initial area of sample cross-section.

Experimental data presented by KWIECIEN and ZAJĄC [20] and KWIECIEN *et al.* [21] for polyurethane material, allow to assume in the identification analysis, as potential candidates, the hyperelastic constitutive models proposed by MOONEY–RIVLIN and OGDEN [6–8]. It is useful to compare these constitutive models with logarithmic model of hypoelasticity. For these descriptions it is possible to define the basic parameters of models, as well as the essential from the point of application of analysed material models, the basic quantities as: initial shear modulus μ_0 , elastic modulus E and Poisson's coefficient ν . For example: initial shear modulus μ_0 is given by: $\mu_0 = 2(C_{10} + C_{01})$ (see e.g. papers [1–10]).

3.3. Introduction of damage

Under repeated tensile or compression strain, many rubber-like materials such as polyurethane (PUR), exhibit a reduction in stress after the initial extension, the so-called Mullins effect or stress-softening, and the mechanism(s) responsible for this is considered to be very important. Damage functions are important tools for analysing the stress-softening materials. In previous isotropic models [4, 5, 14], softening effects are governed by their “damage” functions and their corresponding damage points (sometimes referred to as softening points [5] or maximum-loading parameters [15]). In Sec. 6 we will define a damage function ξ (which may depend on the material properties) such that $0 \leq \xi(x) \leq 1$, $x \in R$ and ξ increases (strictly) monotonically as x moves away from the point $x = 1$, $\xi(1) = 0$.

Before using the proposed model, the two elastic parameters C_{10} and C_{01} and the parameters describing the evolution laws for damage have to be identified. It was performed through uniaxial tension and compression tests results (monotonic for elastic parameters and non-monotonic for damage parameters),

especially by exploiting the shear modulus properties (see Sec. 3.2). Different stages of the procedure are summarized in Sec. 5 and 6. Let us assume that as a first approximation, the term with I_2 has been neglected since the tension test case enables to split the contribution of the two first invariants and moreover, simulation by the Ogden model with only the first invariant and experimental results are in good agreement, also here $\mu_2 = 0$. The behaviour of the elastomers is commonly represented by hyperelastic models, characterized by the strain energy function W , which is often considered to be dependent on the invariants I_1, I_2, I_3 of the Cauchy–Green deformation tensor \mathbf{C} (or another strain tensor). Among the usual hyperelasticity laws (Mooney–Rivlin, Ogden, etc.), the best one for the studied material is the model of Ogden, as shown in Fig. 1. The agreement between experiments and the model is quite good in a monotonic uniaxial tension and compression tests, but for cycle compression tests some phenomena are not taken into account, essentially a decrease of the shear modulus during the cycles and a decrease of the stiffening for high strains, as Figs. 2 and 3 show. The experimental results in a cycle compression test case (realised with some loads and unloadings) are shown in the axes of the engineering stress σ and principal stretch λ . Actually, the occurrence of micro-defects leads to a degradation of the mechanical material properties. Nevertheless it is worthy to note that for a damaged material, the type of load is crucial. In case of tension, the occurrence of micro-defects induces a decrease in the material properties; on the contrary, in case of compression, when the micro-defects are closed, the initial properties are recovered. The model exposed in the Set. 6 takes into account these experimental observations.

4. EXPERIMENTAL UNIAXIAL TENSION AND COMPRESSION TESTS

The material used in this study was a commercial polyurethane material. After compression moulding, the polymer was solidified at a slow cooling rate to ensure that the structure and morphology of the compressed plates will be homogeneous across the thickness and along the length. This material is a two-component elastomer based on main feature of polyurethanes: hard segments A (viscosity 4.40 Pas) and soft segments B (viscosity 0.26 Pas) were compound in and it was combined in proportions 100:10, and the received material had average mass density $\rho = 0.90 \text{ kg/dm}^3$ and hardness under Shore A 55 ± 5 . In the next Sections, in the uniaxial tension identification process, the experimental data of the following tests were accepted: 2R-1, 5R-1 and 7R-1 (paddle sample). In case of uniaxial compression, the following data were used: 9C-1, 7C-1, 6CC-1, 5CT-1, 4C-1, 1C-1, 3CC, 8CZ and 8CG (cylindrical sample with diameter $\phi \approx 46 \text{ mm}$). All investigations were conducted only with quasi-static strain rates. Results of these tests are contained in the report by KWIECIEŃ and ZAJĄC [20] and

published also by KWIECIEŃ *et al.* [21], and are presented in a part in this paper (in Secs. 4.1 and 4.2).

4.1. Tensile test

The stress-strain behaviour of the PUR was determined by means of a INSTRON testing system. The method has been described in detail in the literature. Consequently, only its essential features will be recalled here. Both the quasi-static and dynamic tests were performed at room temperature 295 K. The tensile samples were made from PUR plates. Dog-bone shaped flat specimens were used for the uniaxial tension tests. The length and width of the homogeneous section of the uniaxial tension specimens were 45.0 mm and 17.0 mm, respectively. The specimen thickness was 3.0 mm.

In Fig. 1, the force versus $1/\lambda$ curve is plotted for several tests, and in Fig. 2 the nominal stress versus λ is plotted.

4.2. Compression test

Investigations of compression were performed on disc specimens, cut off from polyurethane plates. The diameter of the specimens was $\phi = 46$ mm and the thickness for the quasi-static compression tests was approximately $H = 50$ mm.

The sample was compressed between two circular dies. The quasi-static compression tests were carried out in a hydraulic testing machine with the rates of deformation equal to 10^{-3} s^{-1} . The surface of each specimen was covered by a thin layer of anti-friction coating before testing. The friction between the sample and the die faces was not accounted for in the true stress-strain calculations because the friction coefficient was likely to be very low (<0.1) between the PUR sample and the steel dies. Consequently, the engineering stress was simply calculated as the load per actual cross-section of the compressed zone: $\sigma = P/(\pi\phi^2/4)$. Three tests were performed for each group of specimens to assure sufficient reliability of the results.

4.3. Typical stress-strain behaviour

The stress-strain relations obtained during uniaxial quasistatic tension of the polyurethane studied are presented in Figs. 3, 4, 5. The curve's number in these pictures indicates the test number. The stress and the strain quantities are referred to the current (instantaneous) value of the specimen cross-section and the thickness values. An example of the stress-strain curves obtained during axial tension of three specimens of PUR subjected to loading with the same strain rate $3 \times 10^{-4} \text{ s}^{-1}$ is shown in Fig. 3. The axial stress vs. axial strain curves shown in Figs. 3–5 were obtained under uniaxial loading at 20°C. The

reproducibility of each curve was checked by three tests performed under the same conditions. This graph is therefore typical for the behaviour of PUR at room temperature. In this part, a simulation of a cycle compression experiment is performed, as described in Fig. 9. Several interesting features deserve attention. First, all experiments showed that the material's behaviour was the same as above (elastic), but nearly incompressible with $\nu \leq 0.499$. As below in Sec. 6, Figs. 7, 8 and 10 show the experimental data for polyurethane in uniaxial cycle compression test as a function of strain intensity measure $\sqrt{M - m}$, or as a function of axial change of length λ for the loading and unloading tests.

5. IDENTIFICATION OF MODELS FOR MONOTONIC LOADINGS

5.1. Outline of the optimization method

The experimental data used in this paper are the data of KWIECIEŃ and ZAJĄC [20] and KWIECIEŃ *et al.* [21] for the uniaxial tension and compression and the numerical values have been obtained from the virgin experimental tables. These data have been used to identify the parameters of the specific strain-energy functions by means of the least squares (LS) technique.

Let $\hat{\lambda} = [\lambda_1^1, \lambda_1^2, \dots, \lambda_1^m]^T$ be the vector of values of a measure of stretch, appropriate to the considered deformation and let $\sigma = [\sigma_1, \sigma_2, \dots, \sigma_m]^T$ be the corresponding values of stress, which may be either nominal stress or Cauchy stress, depending on the deformation. Hence $(\hat{\lambda}, \sigma)$ are the given pairs of data values. The considered material model is represented by the strain-energy function U , from which the stress is calculated and written $F(\hat{\lambda}, \beta) : \mathbb{R} \times \mathbb{R}^n \rightarrow \mathbb{R}$, where $\hat{\lambda}$ takes the values λ_1^i , $i = 1, \dots, m$, and $\beta = [\beta_1, \beta_2, \dots, \beta_n]^T$ is a set of n material parameters to be identified.

Let us define the objective function as the squared 2-norm

$$(5.1) \quad \sum_{i=1}^m (F(\lambda_1^i, \beta) - \sigma_i^{\text{exp}})^2.$$

Hence, the minimization problem is given by

$$(5.2) \quad \min_{\beta} \sum_{i=1}^m (F(\lambda_1^i, \beta) - \sigma_i^{\text{exp}})^2.$$

If $F(\hat{\lambda}, \beta)$ is a non-linear function with respect to β , then a non-linear least squares problem arises.

It is assumed that our material is almost incompressible like majority of the materials with similar elastic properties as rubber.

In the uniaxial deformation tests along the direction-11 we have

$$(5.3) \quad \lambda_1 = \lambda, \quad \lambda_2 = \lambda_3 = \frac{1}{\sqrt{\lambda}}, \quad \lambda = 1 + \varepsilon_1.$$

The invariants of strain in uniaxial tests have the form

$$(5.4) \quad \bar{I}_1 = I_1 = \lambda^2 + 2\lambda^{-1}, \quad \bar{I}_2 = I_2 = \lambda^{-2} + 2\lambda.$$

With a known potential of strain energy it is possible to determine the dependence of the nominal stress as a function of strain. For the model of the Mooney–Rivlin, we have

$$(5.5) \quad \frac{P}{A_0} = 2 \left(1 - \frac{1}{\lambda^3} \right) (\lambda C_{10} + C_{01}) = 2 \left\{ \left(\lambda - \frac{1}{\lambda^2} \right) C_{10} + \left(1 - \frac{1}{\lambda^3} \right) C_{01} \right\},$$

which can be defined in the form

$$(5.6) \quad \frac{P}{2A_0 \left(\lambda - \frac{1}{\lambda^2} \right)} = C_{10} + \frac{C_{01}}{\lambda},$$

where P is the external axial force in the test, A_0 is initial area of cross-section and λ is the coefficient of change of length (stretch). The right-hand side of the above equation is linear with respect to variable $1/\lambda$, what enables preliminary qualification of constants C_{10} , C_{01} . The left-hand side represents equivalent stress. Figure 1 shows this reduced stress change as a function of the reciprocal of the axial stretch for tests 2R-1, 5R-1 and 7R-1. For these tests it has been established that $C_{10} = 0.6832$, $C_{01} = 0.01209$.

In a general formulation for the Mooney–Rivlin model, we can identify parameters C_{10} and C_{01} from the relation

$$(5.7) \quad \frac{P}{A_0} = 2 \left(1 - \frac{1}{\lambda^3} \right) (\lambda C_{10} + C_{01}).$$

The Ogden model introduced generally earlier, in uniaxial tests has now the form:

$$(5.8) \quad \sigma_{11} = \frac{2\mu}{\alpha} \left[\lambda^{\alpha-1} - \lambda^{-1-\left(\frac{\alpha}{2}\right)} \right]$$

and we have to identify two material parameters μ i α .

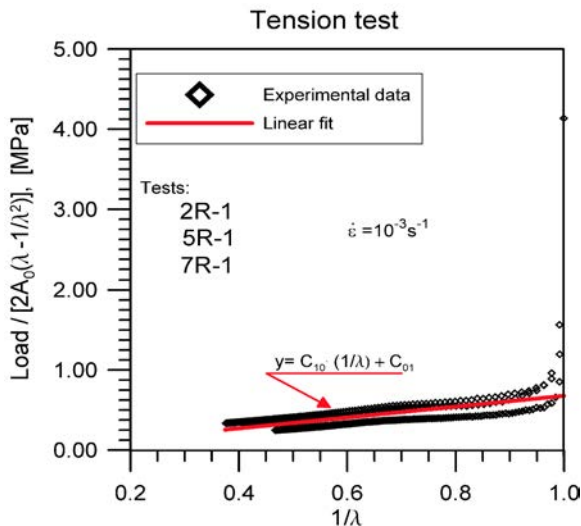


FIG. 1. Dependence of the change of reduced stress $\frac{P}{2A_0 \lambda - \frac{1}{\lambda^2}}$ as a function of the reciprocal of the relative axial stretch $\frac{1}{\lambda}$ in uniaxial tension. Experimental data from KWIECIEŃ *et al.* [20, 21].

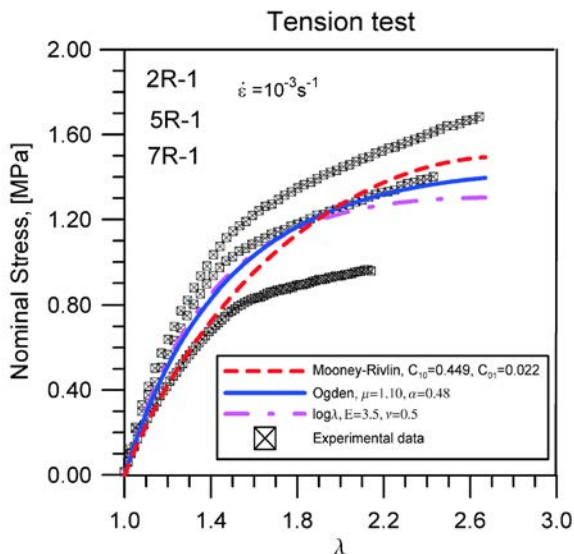


FIG. 2. The nominal stress as a function of the axial stretch λ for polyurethane rubber in a uniaxial tension test, with strain rate $3 \times 10^{-4} \text{ s}^{-1}$ for different constitutive models relations Eqs. (3.6), (3.8), (3.12) (broken and solid lines). Experimental data (quadrates) from KWIECIEŃ *et al.* [20, 21].

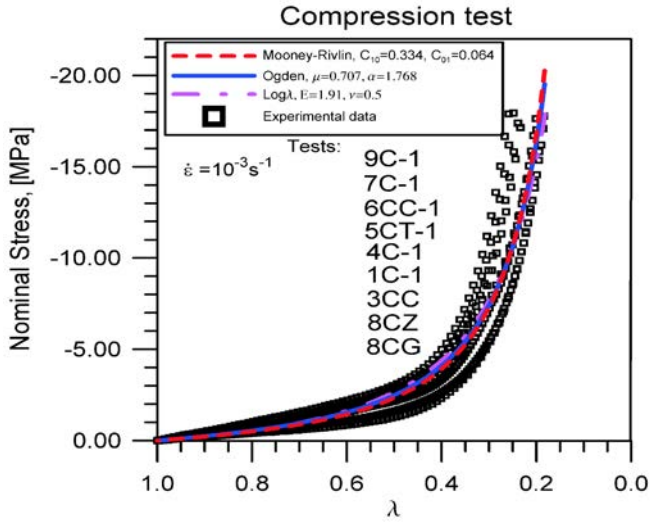


FIG. 3. The nominal stress as a function of the axial stretch λ for polyurethane rubber, in uniaxial compression test with strain rate $3 \times 10^{-3} \text{ s}^{-1}$ for different constitutive models relations Eqs. (3.6), (3.8), (3.12) (broken and solid lines). Experimental data (quadrates marks) from KWIECIEŃ *et al.* [20, 21].

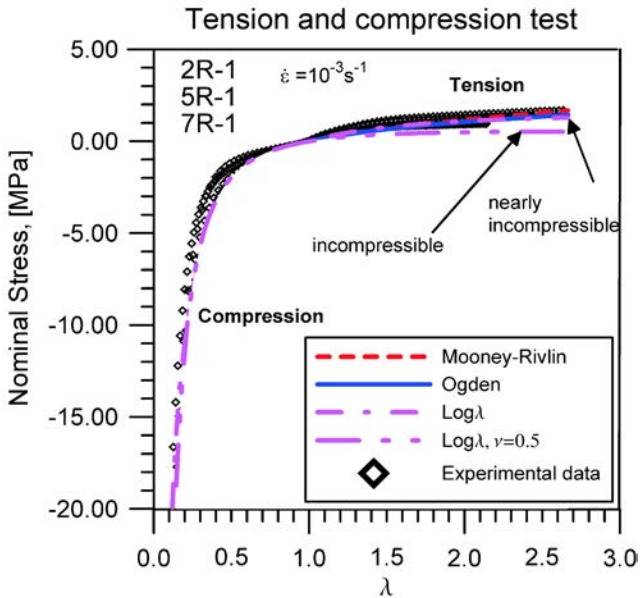


FIG. 4. The nominal stress in uniaxial tension and compression tests as a function of the axial stretch λ , for different constitutive models, Eqs. (3.6), (3.8), (3.12) (broken and solid lines). Experimental data (diamond marks) from KWIECIEŃ *et al.* [20, 21].

In logarithmic description, in uniaxial tests the following relation is given:

$$(5.9) \quad \frac{P}{A_0} = E (\lambda)^{-2\nu} \ln(\lambda)$$

and we have to identify E and ν .

The results of identification process were obtained for tension and compression tests separately and they are presented in Fig. 2 (for tension) and in Fig. 3 (for compression). The results of simulation plotted in Fig. 2 and in Fig. 3 are compared with experimental results. Quadrate marks are used for experimental data, whereas full lines are used for simulation. Identified parameters differed so much that next test of the same process of identification was undertaken for the same file of data for both tests, to identify for this material the set of parameters independent of the type of test. Results of such identification are introduced in Fig. 4. This curve shows the ability of the rubber elasticity models to estimate the material properties.

6. HYPERELASTIC MATERIAL WITH DAMAGE

6.1. Remarks on the use of damage mechanics to describe the Mullins effect

The phenomenon of internal damage in common engineering solid materials depends upon the specific type of the material considered. In addition, for the same material, damage evolution may take place, initiated by very different physical mechanisms, which mainly depend on the type, rate of loading, temperature, as well as on environmental factors such as exposure to corrosive substances. As mentioned in the Introduction, the Mullins effect in rubber elastic materials is often modelled by means of the CDM. Originally, continuum damage mechanics was based on the definition of effective stress (cf. LEMAITRE and CHABOCHE [59]). This theory assumes that, under loading, the material surface on which internal forces are applied is decreasing because of the emergence of micro-defects and micro-voids. Taking into account these physical considerations, in the case of the Mullins effect in solid rubber, following consequences are introduced for the damage evolution:

1. It was proved experimentally that the Mullins effect recovers with time and that this recovery is highly accelerated by annealing (MULLINS [26]). So, the damage in rubber materials may decrease if the whole life of the material is considered.
2. The damage evolution does not differ under different deformation modes: some authors observed the occurrence of stress-softening under tension and compressive conditions.

3. It is mainly recognized that rupture in rubber parts is not directly related to stress-softening. Therefore, high values of the damage parameter should not be considered as a criterion for rupture or occurrence of cracks.

More precisely, the Mullins effect is not a damage but a stress-softening phenomenon. It is due to the rearrangement of the polymer network under deformation when some links between chains (entanglements), or between chains and reinforcement particles (for example carbon black) are broken (BUECHE [51]). Therefore, it should be stressed that CDM can be used to model the Mullins effect in elastic rubber materials with some restrictions and care.

6.2. Description of microstructure damage

Let us consider an isotropic, homogeneous and incompressible rubber-like material. This material is considered to be hyperelastic and subject to isotropic damage in order to describe the Mullins effect. Consequently, it is defined by the existence of a strain energy function, that depends on the deformation gradient \mathbf{F} and on a scalar damage variable α . This variable characterizes the elastic stress-softening of the material. Taking into account the objectivity requirement, the isotropy and the incompressibility, the strain energy function can be written as

$$W = W(I_1; I_2; \alpha),$$

where I_1 and I_2 are the two first principal invariants of the left Cauchy–Green tensor $\mathbf{B} = \mathbf{F}^T \mathbf{F}$ defined in Sec. 3. The third invariant $I_3 = \det(\mathbf{B})$ is equal to 1 due to the incompressibility assumption.

Consider now that the effective Cauchy stress T^* , which acts on the damaged material, is related to the virgin Cauchy stress T_0 by LEMAITRE and CHABOCHE [59] $T^* = T_0(1 - \alpha)$. In case of three-dimensional continuum, the damage model for Mullins effect was proposed by DE SOUZA NETO *et al.* [11]. In this model, the current value of the engineering stress σ in the stress-softened material is given by

$$\sigma = \xi(\alpha) \sigma_0,$$

where the damage function $\xi(\alpha)$ is a differentiable, nondecreasing function of a damage variable $\alpha \in [0, 1]$. The engineering stress in the virgin material is determined by (cf. DE SOUZA NETO *et al.* [11])

$$(6.1) \quad \sigma_0 = \frac{\partial \psi_0(\mathbf{F})}{\partial \mathbf{F}},$$

where $\psi_0(\mathbf{F})$ is the strain energy function for an isotropic, incompressible hyperelastic solid at the current deformation gradient \mathbf{F} . The relation Eq. (6.1) is valid only during monotonic loading. The strain energy function in Eq. (6.1) can

be considered as a product of the surface reducing parameter $(1 - \alpha)$ and the strain energy function of the virgin undamaged material, denoted W_0 :

$$(6.2) \quad W(I_1; I_2; \alpha) = (1 - \alpha)W_0(I_1; I_2).$$

The damage variable α , or the relative strain measure, is defined by $\alpha = \frac{\psi_0}{D}$, where $D \equiv \max_{0 \leq s \leq t} \psi_0(s)$ is the maximum previous value of the strain energy in a deformation history up to the current time t , and s is a running time variable. The evolution of α variable with the deformation must be specified by an additional constitutive law during the loading, unloading and reloading deformation cycles.

Similarly, like OGDEN and ROXBURGH [19], BEATTY and KRISHNASWAMY [16] introduce a generalized JOHNSON and BEATTY [15] elastic material model of stress-softening. In this model, the Cauchy stress \mathbf{T} during loading of the material is a product of the Cauchy stress \mathbf{T}_0 in an isotropic parent material model and an isotropic scalar-valued damage function $\xi(m)$, that depends on the current value of the magnitude of intensity strain m . At a material point \mathbf{X} , the magnitude of strain intensity denoted by m , is defined by $m = \sqrt{\mathbf{B}\mathbf{B}} = \sqrt{\text{tr} \mathbf{B}^2}$, where \mathbf{B} is the left Cauchy–Green deformation tensor. $\mathbf{B} \equiv \mathbf{F} \cdot \mathbf{F}^T$ and \mathbf{F} is the deformation gradient which, in case of incompressibility, requires $\det(\mathbf{F}) = 1$ for all \mathbf{F} , so that

$$(6.3) \quad \mathbf{T} = \xi(m)\mathbf{T}_0.$$

During loading when m is fixed at its current maximum value, $m_{\max} = \max_{0 \leq s \leq t} m(s)$ and the material is unloaded, the Cauchy stress \mathbf{T}^* in the stress-softening elastic material is given by

$$(6.4) \quad \mathbf{T}^* = \xi(m_{\max})\mathbf{T}_0 = \xi(m_{\max}) \frac{\mathbf{T}}{\xi(m)} = \frac{\xi(m_{\max})}{\xi(m)} \mathbf{T} = \xi(m_{\max}, m) \mathbf{T}.$$

The same relations hold when the Cauchy stress is replaced by the engineering stress. The common feature of virgin material response in the described models is that this response, described by the parent material stress \mathbf{T}_0 , is determined by a standard strain energy function for a perfectly elastic, incompressible and isotropic material, which may be hyperelastic.

The loading, unloading and neutral loading from the obtained maximum value $m_{\max} = M$, require $\dot{m} > 0$, $\dot{m} < 0$ and $\dot{m} = 0$, respectively. Intensity m of tensor \mathbf{B} as a function of invariants I_k ($I_1 = \text{tr}\mathbf{B}$, $I_2 = \frac{1}{2}[I_1^2 - \text{tr}(\mathbf{B}^2)]$, $I_3 = \text{de}(\mathbf{B})$) is given by

$$(6.5) \quad m = \sqrt{I_1^2 - 2I_2}.$$

For all deformations of an incompressible material, we have $I_3 \equiv 1$ and $m \geq \sqrt{3}$, where equality is valid when and only when $\mathbf{B} = \mathbf{1}$. By use of the spectral decomposition of tensor \mathbf{B}

$$\mathbf{B} = \lambda_1^2 \mathbf{e}_1 \otimes \mathbf{e}_1 + \lambda_2^2 \mathbf{e}_2 \otimes \mathbf{e}_2 + \lambda_3^2 \mathbf{e}_3 \otimes \mathbf{e}_3,$$

where λ_i are the principal stretches and \mathbf{e}_i are the associated orthonormal principal directions, the intensity of strain m becomes

$$(6.6) \quad m = \sqrt{\lambda_1^4 + \lambda_2^4 + \lambda_3^4}.$$

We consider, like ELIAS–ZÚÑIGA and BEATTY [17], that the material is an isotropic elastic and incompressible material and is described by a time-independent constitutive equation of the form

$$(6.7) \quad \mathbf{T}_0 = 2 \frac{\partial W}{\partial I_1} \cdot \mathbf{B} - 2 \frac{\partial W}{\partial I_2} \cdot \mathbf{B}^{-1} - p \mathbf{1},$$

in which \mathbf{T}_0 is the Cauchy stress, p is hydrostatic pressure and W is the strain energy function per unit reference volume.

Let us assume that our previous strain attained maximum value $m_{max} = M$ during monotonic loading; in such case the stress-softened material response for subsequent unloading and reloading is defined by

$$(6.8) \quad \mathbf{T}^* = \xi(m(\lambda); M) \mathbf{T}_0.$$

The isotropic scalar-valued damage function $\xi(m(\lambda); M)$, called the softening function at the damage level $m_{max} = M$, is a positive monotone increasing function of the strain intensity in the interval $m \in \{m(\lambda = 1); M\}$ and satisfies the conditions

$$(6.9) \quad 0 \leq \xi(m; M) \leq 1, \quad \xi(M; M) = 1.$$

Damage function ξ is determined by a constitutive equation that describes the evolution of microstructural damage that begins immediately after deformation from the natural, undeformed state of the virgin material. Its value $\xi(\sqrt{3}; M)$ characterizes the extent of damage at M , initiated at $m = \sqrt{3}$.

The relations (6.8) for \mathbf{T}^* and (6.9) for the function ξ show that the virgin material and stress-softened material response values coincide only in the unstressed state $\mathbf{T}^* = \mathbf{T}_0 = \mathbf{0}$ and at each softening point $m = M$; otherwise, the stress-softened material response is everywhere smaller than the virgin material response. The material behaviour described by (6.8) for $m \leq M$ is ideally elastic for both loading and unloading, until the value of m exceeds its maximum

previous value M . Thereafter, the material recalls its virgin material response described by (6.7).

For our rubber elastic material, the ratios of the physical stress components \mathbf{T}^* in the stress-softened material to the corresponding physical components \mathbf{T}_0 in the virgin material, for the given deformation, are determined by the softening function alone.

That is, in accordance with Eq. (6.8) and Eq. (6.9)

$$(6.10) \quad \frac{\mathbf{T}^*_{ij}}{\mathbf{T}_0_{ij}} = \xi(m; M) \leq 1, \quad \text{for } i, j = 1, 2, 3 \quad (\text{no summation}).$$

In Eq. (6.10) the equality holds when and only when $m = m_{\max} = M$.

6.3. The form of damage function $\xi(\sqrt{3}; m)$

For the two-phase material model proposed by Mullins–Tobin in 1957 and analysed also by BEATTY and KRISHNASWAMY [16], each material *point* consists of hard phase and soft phase. The total amount of hard phase in solid rubber is much less than the amount of soft phase present in the amorphous microstructure. ELIAS–ZÚÑIGA and BEATTY [17] and BEATTY and KRISHNASWAMY [16] suppose that stress-softening begins immediately after initiation of loading of the original material when $\lambda = 1$ ($m = \sqrt{3}$). As deformation progresses, the volume fraction $\alpha(\sqrt{3}, m)$ of the initial portion of hard phase is transformed to an equivalent portion of soft phase (the rubbery phase), so that the volume fraction α of soft phase increases monotonically with extension (compression). Following ELIAS–ZÚÑIGA and BEATTY [17] we assume that the initiation of stress-softening is possible to appear only after deformation has reached a threshold value λ_a , say $\alpha(\sqrt{3}, m(\lambda_a)) = 0$ for all $\lambda \leq \lambda_a$ and for all $m \leq \sqrt{3}$ we have $\alpha(\sqrt{3}; \sqrt{3}) = 0$. Then the degree of softening of a original material subjected to a maximum previous strain $m_{\max} = M$ is determined by the volume fraction $\alpha(\sqrt{3}, M)$ of hard phase that is transformed by deformation to the new soft phase. During deformation of material $m > \sqrt{3}$, our stress-softening measure $\alpha(\sqrt{3}, m)$ is related to our softening function $\xi(\sqrt{3}, m)$ with the properties described by Eq. (6.8) as follows:

$$(6.11) \quad \alpha(\sqrt{3}; m) = 1 - \xi(\sqrt{3}; m).$$

Relation (6.11) provides a physical basis for the damage function in this theory of stress-softening of rubber-like materials. To determine the softening function from experimental data, the simple relation Eq. (6.10) can be applied to various hypothetical damage functions having the property $0 \leq \xi \leq 1$. In the literature, different forms of damage functions have been introduced for analytical

study, see JOHNSON and BEATTY [15], OGDEN and ROXBURGH [19], DE SOUZA NETO *et al.* [11] or BEATTY and KRISHNASWAMY [16]. JOHNSON and BEATTY [15] suggest for ξ an exponential type function $\xi(\sqrt{3}; m) \equiv e^{-b(m-\sqrt{3})}$, which is studied in several papers, e.g. by BEATTY and KRISHNASWAMY [16], but no direct comparison with experiments is provided. ELIAS–ZÚÑIGA and BEATTY [17] propose an exponential-type equation of law for ξ defined by

$$(6.12) \quad \xi(m; M) \equiv e^{-b\sqrt{M-m}}$$

where b is a positive material constant, named the softening parameter.

The softening function ξ proposed by ELIAS–ZÚÑIGA and BEATTY [17] yields a stress-softening measure α by which the growth of damage may be determined

$$(6.13) \quad \alpha(\sqrt{3}; m) = 1 - \xi(\sqrt{3}; m) = 1 - e^{-b\sqrt{m-\sqrt{3}}}.$$

Application of Eq. (6.13) in Eq. (6.10) determines the stress-softening material model with exponential softening $\xi = e^{-b\sqrt{M-m}}$, for which the stress after unloading follows in accordance with

$$(6.14) \quad \mathbf{T}^* = \mathbf{T}_0 e^{-b\sqrt{M-m}}.$$

The relation (6.14) describes the family of models determined by different values of M which we obtain by describing the elastic, isotropic and incompressible material in the form presented by Eq. (6.7)

During monotonic loading, the strain in material is the actual strain and it is the maximum of strain and $\mathbf{T}^* = \mathbf{T}_0$. If the material is not reloaded again, the strain intensity m decreases from $m = m_{\max}$ and reaction of the material is ideally elastic according to Eq. (6.14) for all $m \leq m_{\max} = M$.

Relation (6.14) or (6.10) after use of logarithm, can be written in the form

$$(6.15) \quad \ln \left(\frac{\mathbf{T}_0}{\mathbf{T}^*} \right) = -\ln \left[\xi(\sqrt{3}; m) \right].$$

The applied theory of rubber-like materials deformation is relatively simple and it is based on purely phenomenological consideration, and identification of the material parameters does not require the measurement of any microscopic quantities. Indeed, behaviour of the material at damaged states is characterized by curves determined from the loading/unloading experiments.

For uniaxial deformation tests of tension and compression, when stretch in axial direction is denoted by $\lambda_1 = \lambda$ with condition of incompressibility $\lambda_1 \lambda_2 \lambda_3 = 1$, we can determine $\lambda_2 = \lambda_3 = 1/\sqrt{\lambda}$.

For the Mooney–Rivlin model, nominal stress $\boldsymbol{\sigma} = \frac{\mathbf{T}_0}{\lambda}$ for monotonic loading is described by Eq. (6.8) and it is obtained for axial loading in the form:

$$(6.16a) \quad \sigma_{11} = 2 \left\{ \left(\lambda - \frac{1}{\lambda^2} \right) C_{10} + \left(1 - \frac{1}{\lambda^3} \right) C_{01} \right\},$$

for monotonic loading and

$$(6.16b) \quad \sigma_{11}^* = 2 \left\{ \left(\lambda - \frac{1}{\lambda^2} \right) C_{10} + \left(1 - \frac{1}{\lambda^3} \right) C_{01} \right\} \xi(m; M),$$

for stress-softening loading, where current value of $m = m(\lambda)$ and maximum value of m , $M = m(\lambda_{\max}) = m(\Lambda)$ before unloading is calculated in accordance with:

$$(6.17) \quad m = \sqrt{\lambda^4 + \frac{2}{\lambda^2}}, \quad M = \sqrt{\Lambda^4 + \frac{2}{\Lambda^2}},$$

where $\Lambda = \lambda_{\max}$ and $M(\lambda_{\max})$ for our experimental compression test $M = 6.21$.

6.4. The identification procedure of parameters of damage function $\xi(m; M)$

Experimental data of stress-softening elastic material response in a strain-controlled test may be used to determine the specific form and all parameters of the softening functions. We shall use only the isotropic scalar function, and this form will only require a small number of equations to be solved when a curve-fitting method is used to obtain its parameters values.

As it is seen in Fig. 5, both models of Mooney–Rivlin show a reasonably good agreement with the experimental data – not only for the primary loading path but also for the reloading paths for the chosen three deformation cycles. In Fig. 5 solutions for both models with identified values of material parameters for three deformation cycles are also shown. It appears that none of these two models gives satisfactory prediction for the three deformation cycles. Naturally, when more deformation cycles are included in the analysis, values of the softening parameters can be better adjusted with the hope of obtaining better fitting of the data. However, no satisfactory prediction can be obtained in this way. The softening functions in the form of Eq. (6.12) proposed by ELIAS–ZÚÑIGA and BEATTY [17] or Eq. (6.13), also fail to give fully satisfactory coincidence of the experimental and theoretical results. The magnitude of softening function $\xi = 1 - \alpha$, shows a strongly non-monotonic behaviour in the characteristic S-shaped form. Variations in shapes of the curves for different deformation cycles show that different values of the softening parameters are needed to fit the experimental data for a particular choice of the softening function. Otherwise more

softening parameters may be needed for definition of this function. In Fig. 7 the softening functions Eq. (6.12) and Eq. (6.13) which were used in fitting the KWIECIEŃ and ZAJĄC [20] or KWIECIEŃ *et al.* [21] data, are also plotted. Differences in shapes of the softening function curves and data curves are striking and this explains the difficulties in fitting experimental data by theoretical models.

In our identification analysis we have applied the following form of function $\xi(m; M)$:

$$(6.18) \quad \xi(\sqrt{3}; m) \equiv e^{-b(M-m)d},$$

where b , M and d are material parameters.

This form of $\xi(m; M)$ requires only two parameters to fit the data via a non-linear least-squares method based on the natural logarithm. For the least-squares method we minimize the expression

$$(6.19) \quad F = \sum_i \left\{ \ln(\xi(m_i; M) \mathbf{T}_0(m_i)) - \ln(\mathbf{T}_{\text{exp}}(m_i)) \right\}^2.$$

The above minimizing statement is equivalent to minimizing

$$(6.20) \quad F = \sum_i \left\{ \ln(\xi(m_i; M)) - \ln \left(\frac{\mathbf{T}_{\text{exp}}(m_i)}{\mathbf{T}_0(m_i)} \right) \right\}^2,$$

which is suitable for the least-square method to obtain the parameters values. We have identified the values of b and d in Sec. 6.7.

6.5. The other forms of damage function $\xi(m; M)$

For better fit we use a new form of ξ function as a combination of two functions, one being (like before) some kind of exponential function $W^*(\lambda)$ and a function $g^*(\lambda)$. Now the function of damage ξ takes the form

$$(6.21) \quad \xi^*(\lambda) \equiv g^*(\lambda)W^*(\lambda) = g^*(\lambda)K e^{-b(\lambda)^d} = (1 - g(\lambda))K e^{-b(\lambda)^d}.$$

The function $g(\lambda)$ in Eq. (6.18) is assumed to be of a logistic form, i.e.,

$$(6.22) \quad g(\lambda) \equiv \frac{g_0}{1 + \exp(F - E \lambda)}$$

where K , g_0 , F and E are material parameters. The form of $W^*(\lambda)$ is known as the Weibull function.

6.6. *The identification of parameters of damage function $\xi(m; M)$ in uniaxial tension test*

In order to determine the material parameters, that appear in the virgin strain energy function W_0 and the evolution equation of the damage variable $\alpha(\lambda)$, uniaxial tensile and cyclic uniaxial compression tests were performed. The uniaxial tensile experiments were conducted on dog-bone flat specimens; the compression test – on specimens which are disc. All experiments were performed under enforced displacement conditions. An example of experimental data is depicted in Fig. 5 for uniaxial tensile tests. In this figure, the experimental stresses are function of principal stretch λ_1 . In experimental tension tests the material was subjected to stretching until achievement of maximum stretching and rupture of sample, and in these tests was not executed the cycle of unloading and reloading. However, let us trace the description of behaviour of such a material also in a situation when the material experienced unloading after achievement of maximum strain just before rupture of the sample. In the case of uniaxial tension it is shown that the Mullins effect can occur almost exclusively during the first loading cycle, and all secondary cycles, i.e. the second, third cycles, are close. Thus, only theoretical stress-softening example which can take place between the first and the third cycles is considered. It is to be noted that reloading paths do rejoin the primary loading curve at the maximum strain. In fact, as the samples are unloaded to zero displacement, they remain in a deformed configuration due to the time-dependent behaviour of the material (creep phenomenon). Consequently, the next reloading stretch level should be higher than the first loading stretch level to rejoin the first path (JOHNSON and BEATTY [15]). As in most of the studies concerning the Mullins effect, the stress-softening behaviour should be separated from other inelastic phenomena, such as hysteresis and relaxation. Concerning the hysteresis phenomenon, unloading paths of cycles are not considered and it is assumed that the equilibrium paths are the loading paths. Nevertheless, the stress-softening model can be developed for loading paths. Once the virgin strain energy function has been chosen, the form of the damage evolution equation (Eqs. (6.12) and (6.18)) has to be established. As detailed in the theoretical part of the paper (Sec. 6.2), the present approach focuses on the use of a measure of deformation expressed as a function of the two first invariants of tensor \mathbf{B} (Eq. (3.1)). As the first approach, we assume a very simple measure of the deformation state that depends only on I_1 :

$$(6.23) \quad m = \sqrt{\lambda_1^4 + \lambda_2^4 + \lambda_3^4}.$$

The damage function $\xi(m; M)$ will be determined using the experimental results. The general method used here is described in Sec. 6.3 without reference to the kind of experiments, but results for uniaxial tensile data are presented.

Consider the experimental results as shown in Fig. 5; the stress-strain relationship reduces to a sequence of loading curves at different maximum strains. For the Mooney–Rivlin model, nominal stress in test of monotonic loading and unloading and cycled reloading and unloading, can be calculated from a formulas given above for the known form of softening function $\xi(m; M)$. For the form of function ξ given by Eq. (6.12)

$$\xi(m; M) = e^{-b\sqrt{M-m}}$$

we define the nominal stress as a function of m .

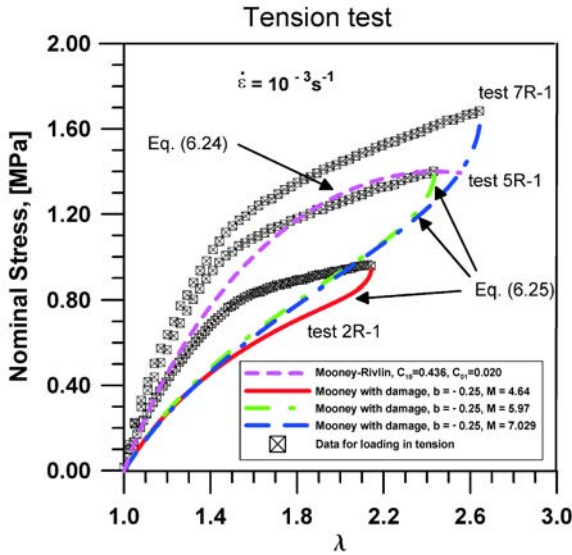


FIG. 5. Nominal stress in uniaxial tension test as a function of axial change of length λ for loading test (experimental data) and relation Eq. (6.24), and three expected paths of unloading from the states with maximum intensities of strain M , defined just before rupture $\lambda = \lambda_{\max}$, for different samples described by Eq. (6.25) with the same damage parameter b .

In this figure, the nominal stress σ is given as a function of the first invariant I_1 . Two types of stress-strain curves can be identified: the primary curve represented by a dashed line and secondary curves represented by solid lines. Depending on the type of curve, the stress-strain relationships are different:

- for the primary curve, the current stress σ_{11} is given by

$$(6.24) \quad \sigma_{11} = 2 \left\{ \left(\lambda - \frac{1}{\lambda^2} \right) C_{10} + \left(1 - \frac{1}{\lambda^3} \right) C_{01} \right\},$$

for monotonic loading, and

- for the i -th secondary curve

$$(6.25) \quad \sigma_{11}^* = 2 \left\{ \left(\lambda - \frac{1}{\lambda^2} \right) C_{10} + \left(1 - \frac{1}{\lambda^3} \right) C_{01} \right\} e^{-b\sqrt{M-m}},$$

for unloading and reloading.

Parameters C_{10} and C_{01} were identified for monotonic loading and accepting $\lambda = \lambda_{\max}$ for each sample and with Eq. (6.17) for m and M . For one cycle of loading it was possible to identify for this model of material with damage of microstructure, one parameter of damage b .

The results of process of identification have been presented in Fig. 5.

6.7. The identification of parameters in compression test

In compression tests the material was subjected to cyclic loading and unloading. Displacement of the upper surface of a cylindrical sample as a function of time is presented in Fig. 6.

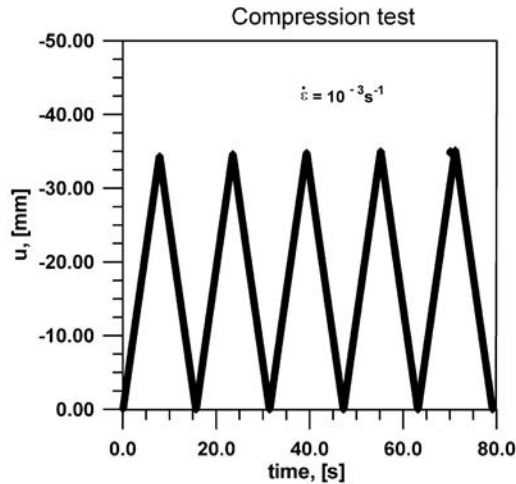


FIG. 6. Change of displacement of the top surface central point of a sample as a function of time in uniaxial quasi-static compression test. Experimental data for samples 6CC-1, cf. [20].

Similarly to the case of tension, let us use the Mooney–Rivlin model for determination of the nominal stress in monotonic loading and cycle unloading and again loading, with the same damage function $\xi(m; M) = e^{-b\sqrt{M-m}}$.

We define nominal stress by the formula similar to that of the tension tests:

$$(6.26) \quad \sigma_{11} = 2 \left\{ \left(\lambda - \frac{1}{\lambda^2} \right) C_{10} + \left(1 - \frac{1}{\lambda^3} \right) C_{01} \right\},$$

for monotonic loading, and

$$(6.27) \quad \sigma_{11}^* = 2 \left\{ \left(\lambda - \frac{1}{\lambda^2} \right) C_{10} + \left(1 - \frac{1}{\lambda^3} \right) C_{01} \right\} e^{-b\sqrt{M_c - m}},$$

for unloading and reloading.

In compression tests parameter C_{10} and C_{01} were also identified like before for monotonic loading and assuming $\lambda = \lambda_{\max}$ and Eq. (6.17) for m and $M_c = M(\lambda_{\max})$. For our experimental compression test $M_c = 6.21$.

Parameter b in the Mooney–Rivlin model can be immediately determined using the relation (6.15) and the results of process of identification for the first and last cycle are presented in Fig. 7.

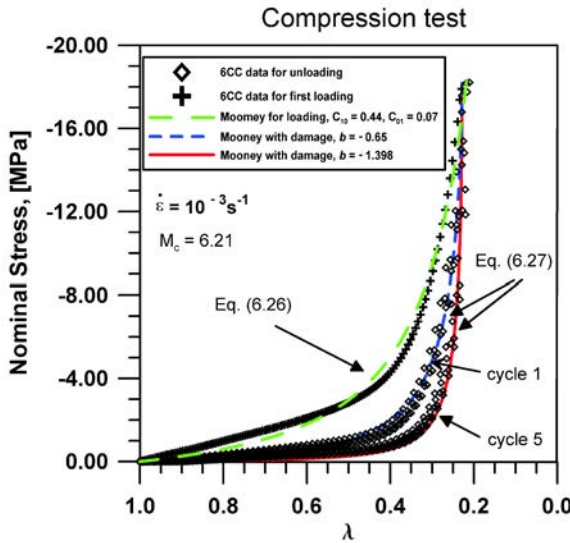


FIG. 7. Nominal stress in uniaxial cycle compression tests as a function of axial change of length λ for loading test (experimental data) and relation Eq. (6.26), and two extreme paths of unloading from the states with maximum intensities of strain M defined for identified models with damaged microstructure described by Eq. (6.27).

Next, we have applied the relation Eq. (6.15) with function $\xi(m; M) = e^{-b\sqrt{M-m}}$ for the first and last cycle and the results of the identification process were presented in Fig. 8.

Now, we applied other forms of the ξ function than that given in Eq. (6.18), to check the possibility of a better fit of models with damage to the experimental data. It is shown that the forms of $\xi(m; M)$ with power $d = 1/2$ and one b parameter can not fit the data for all values of stretches and the values of b are obtained via a non-linear least-squares method based on the natural logarithm. Result for the first and last cycle are presented in Fig. 9.

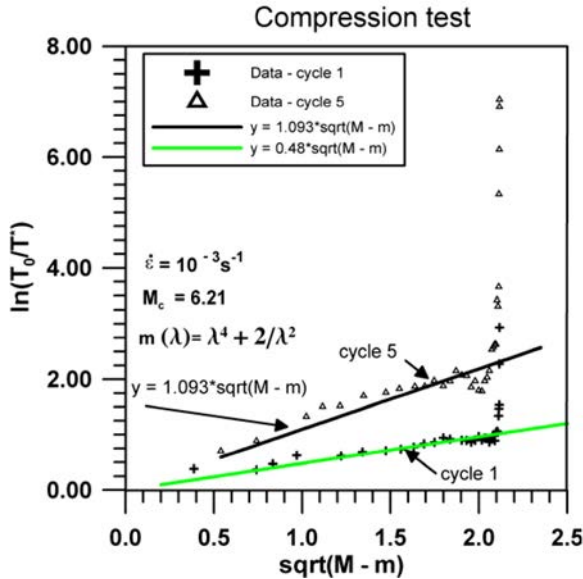


FIG. 8. The value of $\ln \frac{T_{0\ 11}}{T_{11}^*} = \ln \frac{\sigma_{11}}{\sigma_{11}^*}$ in uniaxial compression test as a function of $\sqrt{M - m}$ for unloading test (experimental data) and two extreme values of identified damage parameter b (for first cycle $b = 0.48$ and for last cycle $b = 1.093$) with $M = 1.2$ for one sample.

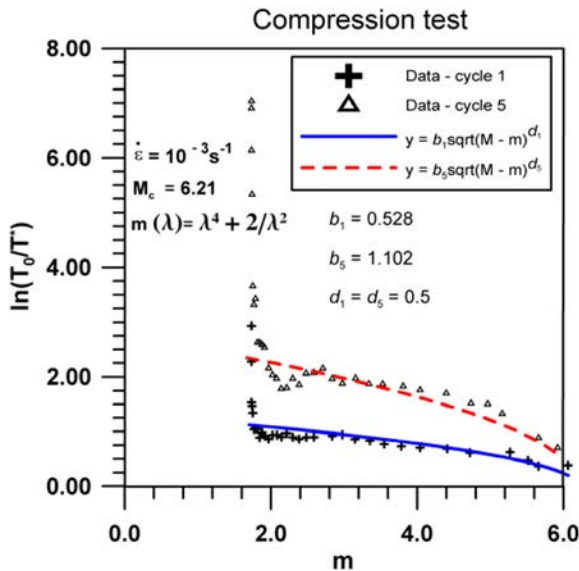


FIG. 9. The value of $\ln \frac{T_{0\ 11}}{T_{11}^*} = \ln \frac{\sigma_{11}}{\sigma_{11}^*}$ in a uniaxial compression test as a function of strain intensity m for unloading test (experimental data), with two identified forms of function $\xi = e^{-b(m-\sqrt{3})^d}$ for extreme cycles of unloading.

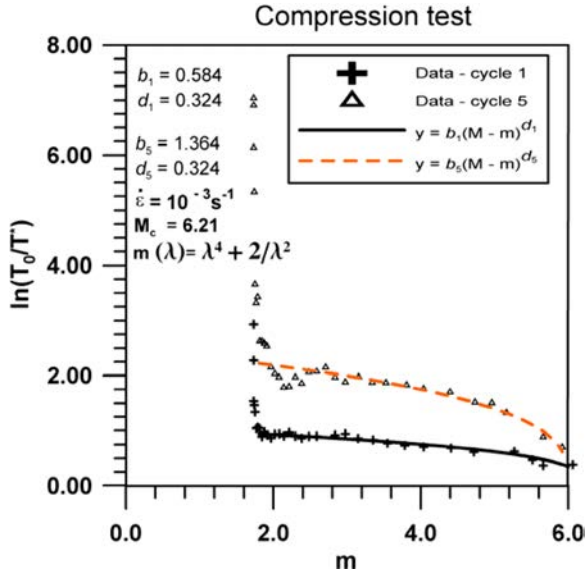


FIG. 10. The value of $\ln \frac{T_{0\ 11}}{T_{11}^*} = \ln \frac{\sigma_{11}}{\sigma_{11}^*}$ in uniaxial compression test as a function of strain intensity m for unloading test (experimental data), with two identified forms of function $\xi = e^{-b(M-m)^d}$ for extreme cycles of unloading.

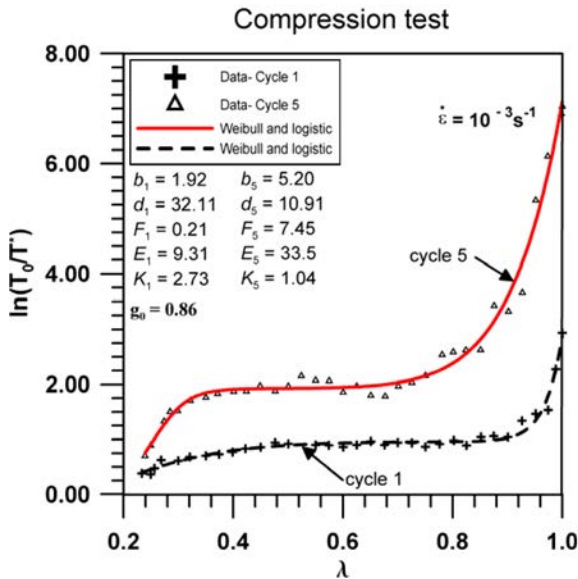


FIG. 11. The value of nominal stress in uniaxial cycle compression tests as a function of axial change of length λ for loading test (experimental data) and two extreme paths of unloading from the states with maximum intensities of strain M defined for identified models with damaged microstructure described by Eqs. (6.21) and (6.22), $\xi^*(\lambda) = K(1 - g(\lambda))e^{-b(\lambda)^d}$.

The identification was performed also for function ξ in the form (6.18)

$$\xi(\sqrt{3}; m) = e^{-b(m-\sqrt{3})^d}.$$

We assume now that the power d in this function can be different than $d = 1/2$. The identification results indicate that the best fitting is obtained with $d = 0.324$. Results of our model adjustment to experimental data for such function ξ are presented in Fig. 10.

The results of identification process for a new function $\xi^*(\lambda)$ given in Eq. (6.21) and Eq. (6.22) for the first and last cycle are presented in Fig. 11.

It is evident that this form of $\xi^*(\lambda)$ with four parameters fitting the data can be also obtained via a non-linear least-squares method, based on the natural logarithm and the results of our model adjustment to experimental data [20, 21] for rubber-like material.

6.8. Comparison of model prediction with experiment

The results of simulation for a tension test are presented in Fig. 1. This figure shows the comparison of the response in terms of force versus inverse stretch ($1/\lambda$) for the classical model of Mooney–Rivlin. Figures 2–4 show the nominal stress as a function of the axial stretch λ .

In the Mooney–Rivlin model for uniaxial tension with stress-softening, four material parameters have to be determined: two for the virgin strain energy, i.e. C_{10} and C_{01} , and two for the evolution equation of the damage, i.e. b and M . Due to the use of a measure of deformation instead of the strain energy function as the damage criterion, the monotonic primary curve could be fitted first by using the data reported in Fig. 5; and then the determination of W_0 reduces to the classical problem of fitting a hyperelastic model, using the primary loading curve. Nevertheless, taking into consideration the limitations discussed above, it is more efficient to perform a global identification using the stress-strain data for both the uniaxial tensile and uniaxial compression tests. For the identification process, the difference between the model and experimental results is calculated simultaneously on all curves. Computations are performed using the known square difference algorithm. The values of material parameters obtained are presented in Fig. 5 and the identification results are compared with experiments.

For uniaxial compression – deformation state, the results are compared with experimental data in Figs. 7–11, respectively. Theoretical results are globally in good agreement with experiments; so, the model describes successfully the transition between different loading curves in cyclic experiments and exhibits the influence of the maximum strain on the softened behaviour. Finally, considering Eq. (6.18) and the values of material parameters given in Fig. 5, the present

approach is applicable until 300% of the deformation in uniaxial tension. In this way, simulation of large strain problems can be considered. This curve shows the ability of the rubber elasticity models to estimate the degradation of the material properties. The stiffening effect for all ranges of strain is here very well estimated. It is important to note that the chosen material function $g(\lambda)$ is a logistic function (see [10, 13]), which is a case of S-shape function and which enables to fit the damage model.

If we compare our theory with the experimental data of MULLINS and TOBIN [24], MULLINS [26] on simple tension and compression as the first step of modelling, we shall only use the isotropic scalar function ξ proposed in Sec. 6, remembering that this form will require only a small number of parameters to be identified, when a curve-fitting method is used, to obtain its parameter values, OGDEN and RUXBURGH [19]. According to [19], the component of the energy function for the original material takes the form $W(\lambda_1; \lambda_2; \alpha) = (1 - \alpha)W_0(\lambda_1; \lambda_2)$.

7. CONCLUSIONS AND FINAL REMARKS

In this paper, the different models proposed in literature for the description of the Mullins effect in rubber-like solids, e.g. the Mooney–Rivlin and the Ogden model, are studied, which are phenomenological in nature, and a microscopically based interpretation of some of the constitutive parameters may be given (see HORGAN and SACCOMANDI [44]). In this way, it was possible to modify a model for the Mullins effect. The mathematical simplicity of the phenomenological models of rubber-like materials allows to determine all their features analytically and to provide new insights into the physical mechanisms underlying the Mullins effect. The solid rubber structures are able to undergo very large deformation up to 300% or 600%, which involves damage of the elastomer. The proposed model, which is based on the continuum damage mechanic, also applied a phenomenological approach, and is simple with few parameters to identify and it is efficient to take into account the degradation of material properties. Moreover, it enables to take into account the asymmetry of the response of the damaged material in tension and compression, which is a worthy aspect to be taken into account in modelling of rubber-like materials. Concerning the simulation, even if the finite element e.g. ABAQUS code enables to perform tension or shear experiment simulation up to higher strains, all the difficulties are not overcome. Of course, one more difficulty is always due to the finite element distortion which could appear when deformation becomes large, even if the sensibility is diminished through the use of a material formulation.

This paper shows that constitutive Eqs. (6.16a) and (6.16b) for axial deformation in tension and compression tests describe the behaviour of the stud-

ied material well, near monotonic as well as cyclic loading. The form of these equations was determined using the model of Mooney–Rivlin for monotonic loading, and the model for cyclic loading proposed by MULLINS and TOBIN [24] and modified by ELIAS–ZÚÑIGA and BEATTY [17], which takes into account the decrease of strength capacity of rubber-like materials under unloading and reloading. The studied material belonging to elastomers material is a two-phase material which consists of hard and soft segments (rubber). Macroscopic behaviour of such materials is the result of conversion of a hard phase into soft phase during deformation and the observed macroscopic growth of the microstructural strains is the result of percentage changes of content of every phase for the given level of macroscopic strain. In the presented models of elastomers, simplified mechanism of deformation is applied, which is mathematically simplified in comparison with the model of non-Gaussian type proposed in papers e.g.: BUECHE [51], GOVINDJEE and SIMO [23]. The well-known in literature, analytical models of Ogden and Mooney–Rivlin hyperelasticity of rubber-like materials are not suitable to describe the behaviour of such materials under reversible loadings. It should be stressed that the applied constitutive description of the interpretation of the experimental results, does not require for each material phase the specification of the constitutive relation. In description of the rubber-like material behaviour under the applied loading it is sufficient to know the constitutive relation for the soft phase. It is also essential, that elastic deformations of hard phase in majority of its volume do not undergo any changes in the process of deformation. The description of mechanisms of influence between the hard and soft phases and conversion of a hard phase into a soft one require, however, additional studies. In paper by GOVINDJEE and SIMO [23] was proposed a certain general explanation of the interaction between phases in the general state of strains, however the analysis of mechanisms of exchange of these phases is missing. It is also justified to consider the additional effects, which have influence on the decrease of strength capacity of rubber-like materials, e.g. such as induced anisotropy (cf. MULLINS [25]). In order to do this, we should consider the effect of arrangement of hard phase as well as suitable growth of the length of free chains network bonds.

Our calculations have shown the efficiency of the models used to simulate the complex phenomena such as the Mullins effect in rubber-like materials. A good compatibility was obtained between the numerical results and the experimentally observed behaviour of polyurethane materials with damages in the finite strains conditions. To determine the proposed phenomenological model of material based on experimental data, we need to identify five constants: C_{10} , C_{01} , M , d and parameter b of softening rate in Eq. (6.5). Different models, e.g. the microstructural model of BEATTY and KRISHNASWAMY [16] or phenomenolog-

ical model of OGDEN and ROXBURGH [19], require considerable calculations to obtain good compatibility with experiment and they require identification of the considerably larger number of material parameters. The models with networks of non-Gaussian distribution of the chains, e.g. the 8-chain Arruda–Boyce model, require identification of only several physical parameters, but these models are not studied in the present paper.

The proposed phenomenological theory of stress-softening behaviour of deformed rubber-like materials described by the constitutive Eq. (6.14) with identified parameters, for the studied material, is suitable for modelling the uniaxial tension and compression tests. For the studied rubber-like material, we can determine constitutive model, as a result of determination of the general form of strain energy density function W , by simple parameters identification. To do this we determine $\frac{\partial W}{\partial I_1} = f(I_1)$ and the identification of parameters is performed by the experiment for uniaxial tension test for $\lambda \geq 1$. Keeping the well-known parameters of function $f(I_1)$, we determine $\frac{\partial W}{\partial I_2} = h(I_2)$ and the identification of parameters can be performed by experiment for the whole range of strains for $\lambda > 0$. The form of strain energy density function W is a result of general form of the Rivlin strain energy density function for hyperelastic material and can be obtained also from different universally applied approximations with application of constants C_{01} and C_{10} . Therefore definite parameters C_{01} and C_{10} for this material can be possibly used in accessible commercial packets of finite elements. In our analysis it was established that the studied rubber-like material, described by the constitutive Eq. (6.14), is characterized in the range of uniaxial tension and compression by the following parameters: $C_{10} = 0.335$ and $C_{01} = 0.00045$ and the estimated initial shear modulus equals $\mu_0 = 2(C_{10} + C_{01}) = 0.67$ [MPa] for the Mooney–Rivlin model with assumption of incompressibility; $\mu = 0.65$ and $\alpha = 1.755$ and estimated initial shear modulus $\mu_0 = \mu = 0.65$ [MPa] for the Ogden model with assumption of incompressibility; Young's modulus $E = 1.41$ [MPa] and Poisson's coefficient $\nu = 0.50$ and the estimated initial shear modulus $\mu_0 = 0.47$ [MPa] for logarithmic model. The assumption of small compressibility improves the agreement of estimations with experiment when Young's modulus $E = 2.44$ [MPa] and Poisson's coefficient $\nu = 0.32$, and the estimated initial shear modulus equals $\mu_0 = 0.942$ [MPa].

Our analysis is limited to the uniaxial experimental tests for this material and the stress behaviour was not studied in more complex deformation states, e.g.: biaxial tension or simple shear. So, we should identify the introduced functions and parameters based on the experimental data for complex states of loading. Such more general verification is required if we would like to apply the modified model for a wide class of hyperelastic materials.

Contrary to observations based on the analysis of experimental data presented in this paper, the softening functions $\hat{\xi} = 1 - \hat{\alpha}(m; M)$ in pseudo-elastic models of the Mullins effect, are always assumed to be monotonously increasing functions of m for all values of the pre-strain M . This is the main reason for the observed qualitative differences in shapes of the softening curves due to theoretical models and the experimental data curves (see Fig. 2 and Fig. 5). This explains also the difficulties in fitting the experimental data by theoretical models. It should be noted further that the modified version of Eq. (6.18) of the virgin softening function Eq. (6.12) can not essentially improve the predictions of pseudo-elastic models of the Mullins effect, because the softening function $\xi(m; M)$ in Eq. (6.18) is also a monotonously increasing function of the axial change of length λ . The predictions of pseudo-elastic models of the Mullins effect with application of the new softening functions Eq. (6.21) and Eq. (6.22) presented in Fig. 11 are very successful.

It is also very important to mention that stress softening is an inherently anisotropic phenomenon, and for description of this we need to understand the method of incorporating the induced anisotropy. However, it has been also pointed out that the anisotropic model cannot be properly developed at the present stage, because suitable experimental data are not available or published. The extension of the results presented here to other states of deformation such as simple or pure shear, is a straightforward matter and the development of a general 3D model presents no conceptual difficulties. So far it has been shown that rubber-like materials constitutive theory is effective due to using the form of energy function given by Eq. (6.2).

ACKNOWLEDGEMENTS

The author is grateful to the State Committee for Scientific Research (KBN, Poland) for its financial support through the grant No. 4 T07E 052 27.

REFERENCES

1. J. LAMBERT-DIANI, C. REY, *New phenomenological behaviour laws for rubbers and thermoplastic elastomers*, Eur. J. Mech. A/Solids, **18**, 1027–1043, 1999.
2. K. FARAHANI, H. BAHAI, *Hyper-elastic constitutive equations of conjugate stresses and strain tensors for the Seth-Hill strain measures*, I. J. Eng. Science, **42**, 29–41, 2004.
3. L. ANAND, *A constitutive model for compressible elastomeric solids*, Computational Mechanics, **18**, 339–355, 1996.
4. MSC. Marc Volume A: *Theory and User Information*, Chapter 7 Material Library, Elastomer, 7-50-7-60.

5. Z. GUO, L. J. SLUYS, *Application of a new constitutive model for the description of rubber-like materials under monotonic loading*, Int. J. of Solids and Structures, **43**, 2799–2819, 2006.
6. R. W. OGDEN, *Large deformation isotropic elasticity – on the correlation of theory and experiment for incompressible rubberlike solids*, Proc. R. Soc. Lond., A **326**, 565–584, 1972.
7. R. W. OGDEN, *Large deformation isotropic elasticity – on the correlation of theory and experiment for compressible rubberlike solids*, Proc. R. Soc. Lond., A **328**, 567–583, 1972.
8. R. W. OGDEN, *Elastic deformations of rubberlike solids*, H.G. Hopkins and M.J. Sewell [Eds.], The Rodney Hill 60th Anniversary Volume (Pergamon, Oxford, UK 328, 499–537, 1982).
9. J. SIMO, R. L. TAYLOR, *Quasi-incompressible finite elasticity in principal stretches. Continuum basis and numerical algorithms*, Comp. Meth. in Appl. Mech. and Eng., **85**, 273–310, 1991.
10. E. M. ARRUDA and M. C. BOYCE, *A three-dimensional constitutive model for the large stretch behaviour of rubber elastic materials*, J. Mech. Phys. Solids, **41**, 389–412, 1993.
11. E. A. DE SOUZA NETO, D. PERIĆ and D. R. J. OWEN, *A phenomenological three-dimensional rate-independent continuum damage model for highly filled polymers: formulation and computational aspects*, J. Mech. Physics of Solids, **42**, 1533–1550, 1994.
12. C. O. HORGAN, R. W. OGDEN and G. SACCOMANDI, *A theory of stress softening of elastomers based on finite chain extensibility*, Proc. R. Soc. Lond., A **460**, 1737–1754, 2004.
13. D. DE TOMMASI, G. PUGLISI and G. SACCOMANDI, *A micromechanics-based model for the Mullins effect*, J. Rheol., **50**, 495–512, 2006.
14. M. M. ATTARD and G. W. HUNT, *Hyperelastic constitutive modeling under finite strain*, I. J. Solids and Structures, **41**, 5327–5350, 2004.
15. M. A. JOHNSON and M. F. BEATTY, *The Mullins effect in equibiaxial extension and its influence on the inflation of a balloon*, I. J. Eng. Science, **33**, 223–245, 1995.
16. M. F. BEATTY and S. KRISHNASWAMY, *A theory of stress-softening in incompressible isotropic materials*, J. Mech. Physics of Solids, **48**, 1931–1965, 2000.
17. A. ELIAS-ZÚÑIGA and M. F. BEATTY, *A new phenomenological model for stress-softening in elastomers*, ZAMP, **53**, 794–814, 2002.
18. A. ELIAS-ZÚÑIGA, *A phenomenological energy-based model to characterize stress-softening effect in elastomers*, Polymer, **46**, 3496–3506, 2005.
19. R. W. OGDEN and D. G. ROXBURGH, *A pseudo-elastic model for the Mullins effect in filled rubber*, Proc. R. Soc. London, A **455**, 2861–2678, 1999.
20. A. KWIECIEŃ, B. ZAJĄC, *Wyniki testów rozciągania, ściskania i ścinania materiału ICOSIT*, Raport KBN (in Polish), Kraków 2006.
21. A. KWIECIEŃ, J. KUBICA, P. STECZ, B. ZAJĄC, *Flexible joint method (FJM) – A new approach to protection and repair of cracked masonry*, First European Conference on Earthquake Engineering and Seismology (a joint event of the 13th ECEE & 30th General Assembly of the ESC), Geneva, Switzerland, 3–8 September 2006, Paper Number: 282.

22. J. C. SIMO, *On a fully three-dimensional finite-strain viscoelastic damage model: formulation and computational aspects*, *Comput. Methods Appl. Mech. Eng.*, 60, 153–173, 1987.
23. S. GOVINDJEE, J. C. SIMO, *A micro-mechanically based continuum damage model for carbon black-filled rubbers incorporating Mullins' effect*, *Journal of the Mechanics and Physics of Solids*, 39 (1), 87–112, 1991.
24. L. MULLINS, N. R. TOBIN, *Theoretical model for the elastic behaviour of filler-reinforced vulcanized rubbers*, [in:] *Proceedings of the Third Rubber Technology Conference, London 1954 (Published in 1956)*, 397–412, 1956.
25. L. MULLINS, *Effect of stretching on the properties of rubber*, *Journal of Rubber Research*, 16 (12), 275–289, 1947.
26. L. MULLINS, *Softening of rubber by deformation*, *Rubber Chemistry and Technology*, 42 (1), 339–362, 1969.
27. C. MIEHE, *Discontinuous and continuous damage evolution in Ogden-type large-strain elastic materials*, *Eur. J. Mech. A/Solids*, 14, 697–720, 1995.
28. C. MIEHE, S. GÖKTEPE, F. LULEI, *A micro-macro approach to rubber-like materials – Part I: the non-affine micro-sphere model of rubber elasticity*, *Journal of the Mechanics and Physics of Solids*, 52, 2617–2660, 2004.
29. C. MIEHE, S. GÖKTEPE, *A micro-macro approach to rubber-like materials. Part II: The micro-sphere model of finite rubber viscoelasticity*, *Journal of the Mechanics and Physics of Solids*, 52, 2231–2258, 2005.
30. S. GÖKTEPE, C. MIEHE, *A micro-macro approach to rubber-like materials. Part III: The micro-sphere model of anisotropic Mullins-type damage*, *Journal of the Mechanics and Physics of Solids*, 53, 2259–2283, 2005.
31. S. KRISHNASWAMY, M. F. BEATTY, *The Mullins effect in compressible solids*, *Int. J. of Eng. Science*, 38, 1397–1414, 2000.
32. B. MEISSNER, L. MATEJKA, *A structure-based constitutive equation for filler-reinforced rubber-like networks and for the description of the Mullins effect*, *Polymer*, 47, 7997–8012, 2006.
33. G. HEINRICH, M. KALISKE, *Theoretical and numerical formulation of a molecular based constitutive tube-model of rubber elasticity*, *Comput. Theor. Polym. Sci.*, 7 (3/4), 227–241, 1997.
34. R. W. OGDEN, G. SACCOMANDI, I. SGURA, *Fitting hyperelastic models to experimental data*, *Computational Mechanics*, 34 (6), 484–502, 2004.
35. R. KAZAKEVICIUTE-MAKOVSKA, *Experimentally determined properties of softening functions in pseudo-elastic models of the Mullins effect*, *International Journal of Solids and Structures*, 44, 4145–4157, 2007.
36. C. O. HORGAN, J. G. MURPHY, *Plane strain bending of cylindrical sectors of admissible compressible hyperelastic materials*, *Journal of Elasticity*, 81(2), 129–151, 2005.
37. Z. P. HUANG, J. WANG, *A theory of hyperelasticity of multi-phase media with surface/interface energy effect*, *Acta Mechanica*, 182 (3–4), 195–210, 2006.
38. C. O. HORGAN, J. G. MURPHY, *Invariance of the equilibrium equations of finite elasticity for compressible materials*, *Journal of Elasticity*, 77 (3), 187–200, 2004.

39. A. DESIMONE, J. J. MARIGO and L. TERESI, *A damage-mechanics approach to stress softening and its application to rubber*, Eur. J. Mech. A, 20, 873–892, 2001.
40. A. LION, *A constitutive model for carbon-black-filled rubber: experimental investigations and mathematical representation*, Continuum Mech. Thermodyn., 8, 153–169, 1996.
41. E. G. SEPTANIKA, L. J. ERNST, *Application of the network alteration theory for modeling the time-dependent constitutive behaviour of rubbers, Part I.*, Mech. Mater., 30, 253–263, 1998.
42. F. ANDRIEUX and K. SAANOUNI, *On a damaged hyperelastic medium: Mullins effect with irreversible strain*, Int. J. Damage Mech., 8, 82–103, 1999.
43. G. MARCKMANN, E. VERRON, L. GORNET, G. CHAGNON, P. CHARRIER and P. FORT, *A theory of network alteration for the Mullins effect*, J. Mech. Phys. Solids, 50, 2011–2028, 2002.
44. C. O. HORGAN, G. SACCOMANDI, *A molecular-statistical basis for the Gent constitutive model of rubber elasticity*, J. Elasticity, 68, 167–176, 2002.
45. H. J. QI and M. C. BOYCE, *Stress-strain behaviour of thermoplastic polyurethanes*, Mechanics of Materials, 37, 817–839, 2005.
46. P. KRÓL, *Synthesis methods, chemical structures and phase structures of linear polyurethanes. Properties and applications of linear polyurethanes in polyurethane elastomers, copolymers and ionomers*, Progress in Materials Science, 52, 915–1015, 2007.
47. C. MIEHE, J. KECK, *Superimposed finite elastic-viscoelastic-plastoelastic stress response with damage in filled rubbery polymers. Experiments, modelling and algorithmic implementation*, J. Mech. Phys. Solids, 48, 323–365, 2000.
48. G. POMPE, A. POHLERS, P. PÖTSCHKE, J. PIONTEC, *Influence of processing conditions on the multiphase structure of segmented polyurethane*, Polymer, 39, 5147, 1998. (280)
49. W. KURAN, M. SOBCEK, T. LISTOS, C. DEBEK, Z. FLORJANCZYK, *New route to oligo-carbonate diols suitable for the synthesis of polyurethane elastomers*, Polymer, 41 (24), 8531–8541, 2000. (42)
50. M. HERRERA, G. MATUSCHEK, A. KETTRUP, *Thermal degradation of thermoplastic polyurethane elastomers (TPU) based on MDI*, Polymer Degradation and Stability, 78 (2), 2002.
51. F. BUECHE, *Molecular basis for the Mullins effect*, Journal of Applied Polymer Science, 4 (10), 107–114, 1960.
52. L. R. G. TRELOAR, *Stress-strain data for vulcanised rubber under various types of deformation*, Trans. Faraday Soc., 40, 59–70, 1944.
53. H. M. JAMES and E. GUTH, *Theory of the increase in rigidity of rubber during cure*, J. Chem. Phys., 15, 669–683, 1947.
54. L. R. G. TRELOAR and G. RIDING, *A Non-Gaussian theory for rubber in biaxial strain. I. Mechanical properties*, Proc. Roy. Soc. London A, 369, 261–280, 1979.
55. H. M. ARRUDA and M. C. BOYCE, *A three-dimensional constitutive model for the large stretch behavior of rubber elastic materials*, J. Mech. Phys. Solids, 41, 389–412, 1993.
56. P. D. WU and E. VAN DER GIESSEN, *On improved network models for rubber elasticity and their applications to orientation hardening in glassy polymers*, J. Mech. Phys. Solids, 41, 427–456, 1993.

57. M. C. BOYCE and E. M. ARRUDA, *Constitutive models of rubber elasticity: a review*, Rubber Chem. Technol., **73**, 505–523, 2000.
58. A. N. GENT, A new constitutive relation for rubber, Rubber Chem. Technol., **69**, 59–61, 1996.
59. J. LEMAITRE, J. L. CHABOCHE, *Mechanics of Solid Materials*, Springer-Verlag, Berlin, 1987.

Received March 22, 2007; revised version December 19, 2007.
